Asian Journal of Chemistry; Vol. 27, No. 8 (2015), 2905-2910

ASIAN JOURNAL OF CHEMISTRY

http://dx.doi.org/10.14233/ajchem.2015.18282

Preparation and Characterization of Two Component Transparent Zinc Oxide/Silicone Nanocomposites for Power Light Emitting Diodes Encapsulant

XIAOYONG HU[1,*], ZHIYUAN LIN[1], YOUMING ZHENG[1] and YUQING XU[2]

[1]College of Biological and Chemical Engineering, Guangxi University of Science and Technology, Liuzhou 545006, Guangxi, P.R. China
[2]College of Materials Science and Engineering, Guilin University of Technology, Liulin 541004, Guangxi, P.R. China

*Corresponding author: Fax: +86 772 3516078; Tel: +86 772 688511; E-mail: hxypym@126.com

Received: 10 June 2014; *Accepted*: 5 September 2014; *Published online*: 27 April 2015; AJC-17161

Novel transparent zinc oxide (ZnO)/silicone nanocomposites for power light-emitting diodes packaging with excellent properties including a high transparency, UV-shielding efficiency and thermal properties were successfully synthesized through a three-step reaction routes: (i) ZnO precursor was prepared *via* homogeneous precipitation method and ZnO nanpoparticles were then obtained by calcination of the precursor at different temperature; (ii) the graft polymerization of surface fractionalized ZnO (m-ZnO) nanoparticles in hydrogen-containing poly(methysiloxane) were investigated and then mixed with terminal-vinyl poly(methylsiloxane) and MQ silixone resin as component B; (iii) the hydrosilylation chemistry of terminal-vinyl polymethysiloxane (as component A) in (ii) with MQ silicone resin and platinum catalysts. The structural properties of the as-prepared ZnO nanoparticles were studied and the nanocomposites were characterized through Fourier transform infrared, themogravimetry and Scanning electron microscope. The optical properties of nanocomposites namely visible light transparency and UV-light shielding efficiency were studied using an ultraviolet-visible spectrophotometer. The results indicated that functionalizations with A151 greatly improved the dispersion of ZnO in silicone due to their high chelating capacities with ZnO and the refractive index of m-ZnO in nanocomposites were changed by chemical grafting. The optical properties of the as-obtained nanocomposites were shown to depend on ZnO particle size and the nanocomposites containing 0.06 % in weight of functionalized ZnO nanoparticels with an average particle size of 96.01 nm after calcination at 400 °C possessed excellent visible-light transparency and high UV-light shielding deficiency. Moreover, the thermal properties of nanocomposites was enhanced with m-ZnO introduced and met the requirements of high-performance electronic packaging for high-power light-emitting diodes encapsulant.

Keywords: ZnO Nanoparticles, Nanocomposites, Optical properties, Thermal properties.

INTRODUCTION

In recent years, power light-emitting diodes have been called as "green solid-state lighting" that are proposed for specially lighting applications due to its superior characteristics such as high energy efficiency, reliability and environmental-friendly properties[1,2].

Packaging technology is one key and an indispensable step for the practical application of light-emitting diodes lighting[3]. Traditional epoxy resins as packaging materials have been most frequently employed in low-power light-emitting diodes technology because of their electrical insulation, standard processability and low cost[4,5]. However, as high-power white light-emitting diodes attracted considerable attention, epoxy resins encountered the disadvantages of being poor not only in thermal resistance caused by high-heat radiation, but also being poor in light resistance as a result of low transmittance for a stronger short-wavelength radiation. This means that the lifetime and luminous efficiency of a high-power light-emitting diodes tend to be easily weakened by heat and UV-radiation[6,8]. Therefore, to met requirements of packaging material for high-power white light-emitting diodes, it should not only possess a high thermal resistance and thermal conductivity to prevent heat accumulating, but should also maintain a high UV-light shielding, visible-light transparency and UV-irradiation resistance. The reliability of those is becoming an urgent issue for the emerging illumination applications.

Instead of conventional epoxy resins, the transparent silicone resins as novel packaging materials showed great potential for standard high-power white light-emitting diodes packaging because of their excellent transparency, low moisture absorption and high thermal stability[9,10]. However, silicone resins do not filter UV-rays which may leak out from the high-power light-emitting diodes to harm human skins or eyes[11]. Hence, it is necessary to develop truly multifunctional transparent silicone composites with outstanding UV-shielding capability. Numerous studies demonstrated that through the incorporation of inorganic nanoparticals[12-14], such as SiO_2, TiO_2 and Al_2O_3 to

polymer could be enhanced significantly UV-light resistance and UV-light shielding. Moreover, transparency could be maintained when the refractive index of the particle fillers were approximately equal to that of polymer and in nanometer with low content[15]. Zinc oxide is an outstanding inorganic material closely related with ultraviolet light and shows a potential application in transparent polymer as UV-light filters due to its extremely high thermal conductivity, UV-shielding efficiency and low refractive index. In addition, it had been proved that ZnO/epoxy and ZnO/poly (styrene butylacrylate) latex nanocomposites exhibited high UV-shielding efficiency[16,17]. However, the preparation of ZnO/silicone nanocomposites as packaging materials for high-power white light-emitting diodes was reported rarely and this is a kind of trend that well worth to studying. It was reported that the refractive index of transparent silicone (1.56) was lower than that of ZnO (2-2.13)[18]. It means that is mismatching of refractive indexes of nano-ZnO and silicone matrix. Moreover, the effect of scattering reflection is ignorable when the particle size of filler is much smaller than the wavelength of the incident light. However, if ZnO nanoparticles are too small they would bring about blue-shift and morover nanoparticles with high surface energy, which finally tend to aggregate into large particles and cause light scattering and hence reduce UV-shielding efficiency[15,19].

In the previous research, many attempts have been made to improve the dispersion and bonding of filler in matrix by surface treatment of nano-ZnO filler with different chemicals, such as organic fluorine[20], sodium dodecyl sulfate (SDS) and silane, *etc*.[21,22]. However, all of them were indicated that the comprehensive performance of nanocomposites were decreased due to the poor stability of nanoparticles as it used for a long time. In this paper, a new method to prepare high-performance ZnO/silicone nanocomposites for high-power light-emitting diodes packaging was developed. The surface of nano-ZnO particles were pre-treated by vinyl-triethoxysiliane and then the compatibility and refractive index between ZnO nanoparticles and silicone substrate were improved *via* the method of chemical grafting. The effects of ZnO particles size, surface nature and content on the optical and thermal properties of ZnO/silicone nanocomposites were investigated. We expected to develop a novel packaging materials for high-power white light-emitting diodes.

EXPERIMENTAL

Zinc nitrate hexahydrate [$Zn(NO_3)_2{\cdot}6H_2O$] was purchased from Xilong Chemical Co., Ltd. Vinyl-triethoxysilane (A-151) was purchased from Nanjing Qianxiang Chemical Co., Ltd. Vinl-containing MQ-silicone resin was purchased from Guangzhou Xinhua Silicone Co., Ltd. Platinum catalysts were purchased from Shenzhen Lianhuan Silicone Material Co., Ltd. Vinl-containing polymethylsiloxane (PVMS) and hydrogen-containing polymethylsioxane (PHMS) were obtained from Guangzhou Jinguige Silicone Co., Ltd. All other chemicals were commercially available and used as received.

Synthesis of ZnO nanoparticles: ZnO nanoparticles were synthesized by a precipitation method and the specific procedure was as follows: $Zn(NO_3)_2{\cdot}6H_2O$ (20 g) dissolved in 150 mL deionized water with A151 (0.5 g) was marked as solution A and Na_2CO_3 (13 g) dissolved in 200 mL deionized water was marked as solution B. Solution A was added to solution B drop by drop and vigorous stirred at 45 °C for 6 h. The resulting white precipitates were separated by centrifuge, washed with deionized water and absolute ethanol for three times. The solids were then dried at 100 °C for 5 h in a vacuum system to remove the solvent. Finally, ZnO nanoparticles were obtained after calcination of the solids in air at 100, 200, 300, 400, 500 and 600 °C for 2.5 h, respectively and they were denoted as Z_1, Z_2, Z_3, Z_4, Z_5 and Z_6, respectively.

Chemical grafting of PHMS with m-ZnO: The small amount of ZnO particles were dispersed into 10 mL methyl benzene by centrifuge and then were mixed with A-151 (0.1 g) under stirring at 55 °C for 1 h to pre-treatment on the surface of particles (they were denoted as m-Z_x), then cooled down to 40 °C and PHMS (3 g) with dibutyl tin-dilaurate (0.05 g) were added and the mixture was refluxed under vigorous stirring for 2 h with N_2 protection. The reaction mixture was cooled down to room temperature, the product was collected by vacuum distillation and deformation. the graft copolymer was coded as ZnO-PHMS. And then it will mixed with PVMS and MQ silicone resin as component B.

Preparation of ZnO/silicone nanocomposites: The methyl-vinylsilicone MQ resin, A151 and platinum catalyst were added into PVMS with stirring under vacuum and the mixture was marked as component A. And then component B (the curing agent) was added into component A with vigorous mixing in a vacuum mixer until a homogeneous mixture was obtained. After the mixture was treated *via* ultrasonic and vacuum, poured it into mold and followed bu curing at 150 °C for 2.5 h in a vacuum oven. After this curing process, the samples were removed from the mound. Fig. 1 shows the schematic diagram of ZnO nano particles chemical grafting with silicone polymer.

The generated ZnO were characterized by X-ray diffraction (XRD, DX-2700). Fourier transform infrared spectra (FT-IR, VERTEX 7.0) were recorded at ambient temperature using a Bin-Rad spectrometer (Model Win-IR). Morphological structures of the as-prepared surfaces were observed by digital scanning electron microscopy (SEM, S-3400N). The optical properties were studied with an ultraviolet-visible (UV-visible, UV-2102PC) spectrophotometer and then the absorbance and transmittance spectra were scanned in the range 200-800 nm with a 2 nm interval. Thermal analysis was performed using a Universal V2.6TG-TA Instrument in a nitrogen atmosphere in the temperature range of 50-800 °C and at the heating rate of 10 °C/min.

RESULTS AND DISCUSSION

The preparation of the ZnO precursor by using the homogeneous precipitation method was reported in this work. ZnO nanoparticles were then obtained after calcination of the precursor in air at 100, 200, 300, 400, 500 and 600 °C for 2.5 h, respectively, as showed in Table-1.

Fig. 2 presents the XRD patterns of several ZnO nanoparticles prepared at different calcination temperatures. As shown in Fig. 2, all the particles show a hexagonal Wurtzite

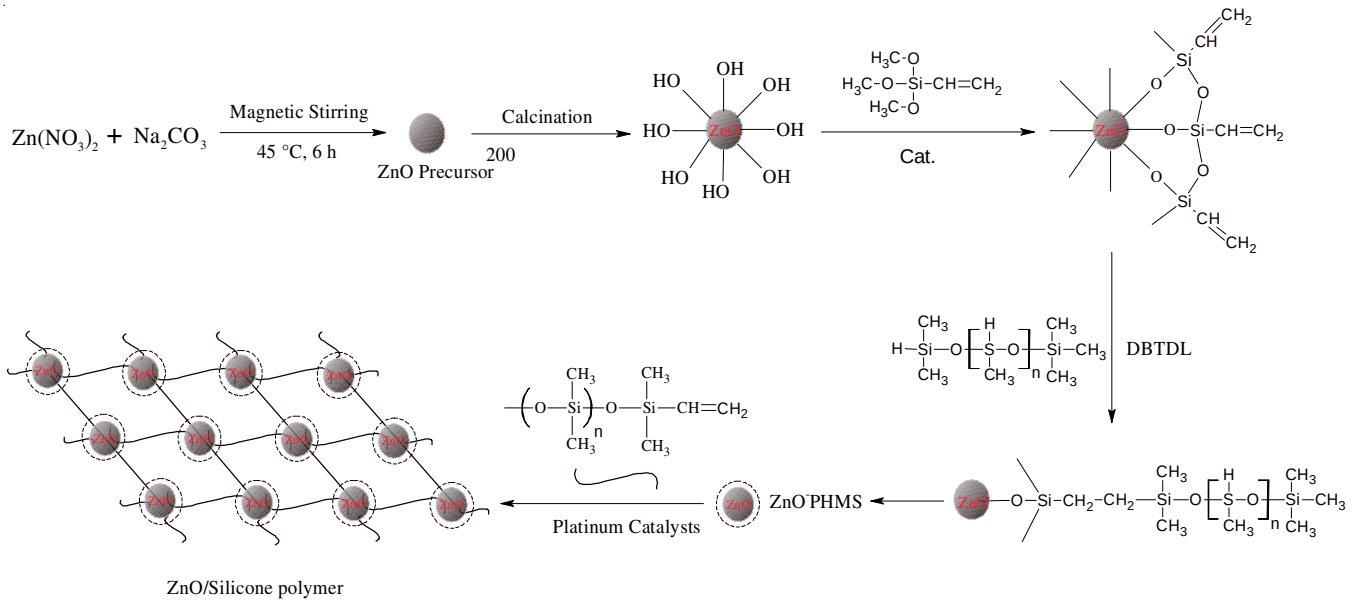

Fig. 1. Schematic diagram of m-ZnO particles grafting with silicone polymer

TABLE-1
PREPARATION OF ZnO NANOPARTICLES BY CALCINATION OF PRECURSOR AT DIFFERENT TEMPERATURES FOR 2.5 h

Sample code	Z_1	Z_2	Z_3	Z_4	Z_5	Z_5
Calcination temperature (°C)	100	200	300	400	500	600

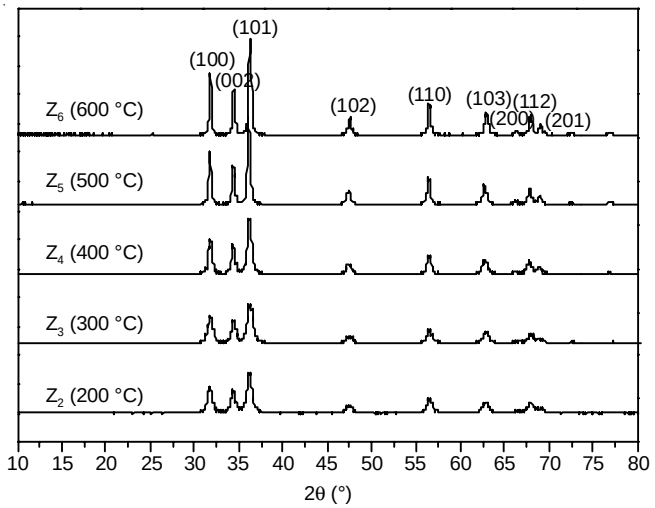

Fig. 2. XRD patterns of ZnO prepared at different calcination temperatures

crystal structure, which is assigned by comparing the diffraction peak positions with those report in the international center for diffraction data table for a standard ZnO powder[23]. On one hand, no diffraction peaks are observed from other phased of ZnO or impurities in Fig. 2. On the other hand, the XRD patterns of ZnO clearly indicate that the diffraction peaks tend to move toward lower angle and became more intensive and this is because the degree of crystallization lattice are enhanced and there are no other residual impurities with increasing calcination temperatures. This is also confirmed by FT-IR in Fig. 3a. The FT-IR spectrum of as-prepared ZnO exhibits an obvious band at 510 cm^{-1} after calcination of the precursor and the shoulders of ZnO stretching peaks in the range[16] of 1200-500 cm^{-1} are disappeared as the calcination temperature increases, which is consistent to XRD result. It is concluded that ZnO nanoparticles are synthesized through this method.

Moreover, Fig. 3b also displays the FT-IR spectra of the original and modified ZnO particles by A151 couping agent. The two absorption bands at 2921, 2846 cm^{-1} can be ascribable to the -CH_2- symmetric and un-symmetric stretching vibration peaks[25] and band at 1402 cm^{-1} is attributable to the -CH=CH_2 absorption peaks[26]. The other absorption bands at 725 cm^{-1} is due to the stretching vibration of -Si-O- groups[27]. The results further confirm that the A151 have been successfully self-assembled or adsorbed onto the ZnO particles. A151 has a very low surface energy and can effectively improve the free energy of the ZnO surfaces and this is also proved by SEM and contact angle measurement in Figs. 3 and 6.

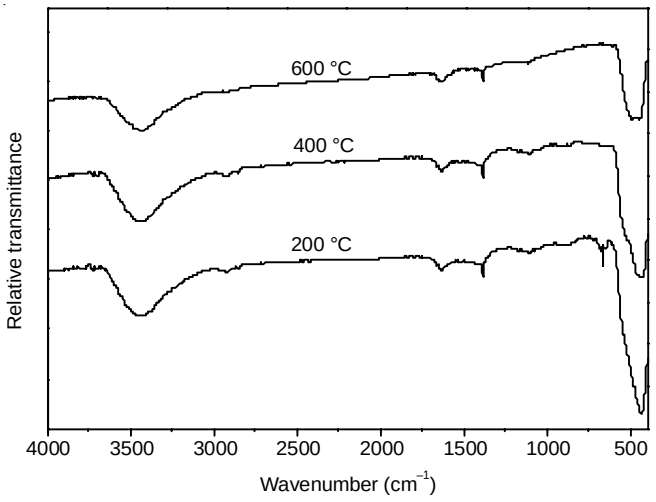

Fig. 3. FT-IR spectra of various samples

Further morphological and structural characterization of as-synthesized ZnO obtained by calcination procedure in air at different temperatures were performed by using SEM and section are displayed in Fig. 4 (Z_3-Z_5 and m-Z_4). As shown in Fig. 4, ZnO nanoparticles calcined at low temperature has some

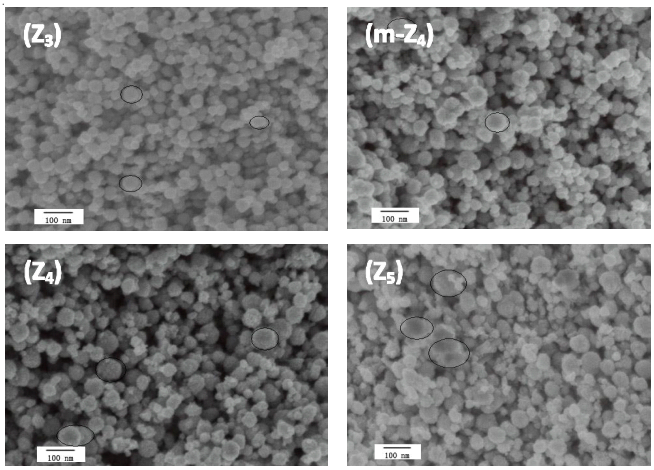

Fig. 4. SEM microphotographs of various ZnO nanoparticles (Z_3-Z_4)

variable fine particle sizes (Z_3). However, the particle sizes are gradually increased with increasing calcination temperature and some agglomerates can be observed. This is because when ZnO particles synthesized at calcination temperature higher than 400 °C (Z_4), the morphology of the ZnO nanoparticles change from a homogeneous spherical shape to a mixed morphology consisting of short prismatic-s, hexagons and quasi-sphericity, which is also consistent to XRD result.

The ZnO crystallite sizes are calculated with Scherrer's formula[24] and the results are given in Table-2. Clearly, an increase in calcination temperature brings about a corresponding increase on crystallite size, leading to sharper diffraction peaks.

TABLE-2
MEAN SIZE OF THE ZnO NANOPARTICLES ESTIMATED USING THE XRD TECHNIQUE AND SCHERRER'S EQUATION

Sample code	Z_2	Z_3	m-Z_4	Z_4	Z_5
Mean particle size (nm)	93.75	108.27	96.01	137.25	199.26

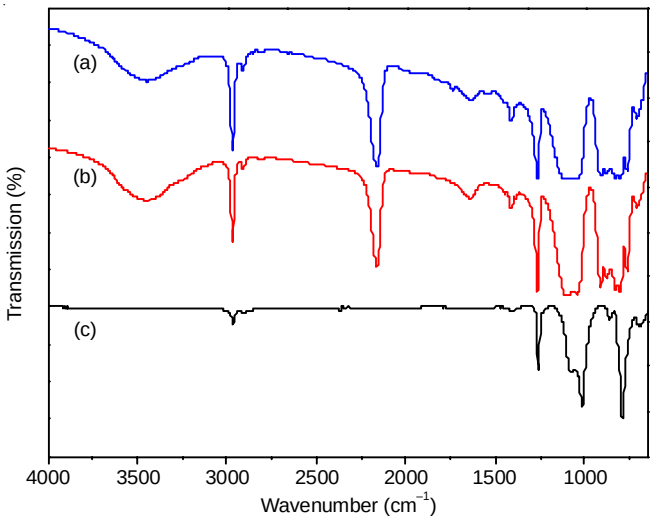

Fig. 5. FT-IR spectra of various samples: (a) PHMS (b) ZnO-PHMS (c) nanocomposites

ZnO-PHMS as curing agent was prepared by chemical grafting and transparent ZnO/silicone nancomposites were synthesized from component A and component B *via* in hydrosilylation reaction. This process could be proved by FT-IR analyses. Fig. 5 shows FT-IR spectra of PHMS, ZnO-PHMS and nanocomposites (0.06 wt % m-Z_4). These three spectra are similar and all of them have a strong shoulder in 1013 cm^{-1} region that are the typical asymmetrical stretching vibration absorption peaks of Si-O-Si groups. In addition, the -CH=CH_2 groups and -Si-H originated, respectively from the structures of PVMS and PHMS at 1678 and 2163 cm^{-1} are almost totally disappeared after the complete curing as well[28] and showed in Fig. 5c. It is illustrated that the curing reaction of the nanocomposites are relatively completed under the curing conditions of 150 °C for 2.5 h. Simultaneously, to compare with unmixed silicone, it also clearly show that the two absorption bands at 2917 and 2848 cm^{-1} (-CH_2- symmetric stretching vibration peaks) are disappeared and a new absorption band at 862 cm^{-1} (in Fig. 5b c) can be attributable to the characteristic stretching vibration peak of -Si-O-Zn covalent bond[29]. These results indicate that ZnO nanoparticles are successfully grafted into silicone chain by chemical method, not modified by physical blend.

Fig. 6 shows the SEM micrographics of nanocomposites modified by chemical grafting and physical blend. As can be seen from the Fig. 6a-c, the modification of nancomposites visible, chemical grafting method exhibited more higher excellent smoothness, lighting and hydrophobic than that of curing by physical bleeding in Fig. 6d-f. This is because of the nano-ZnO physical blending reunion phenomenon is seen.

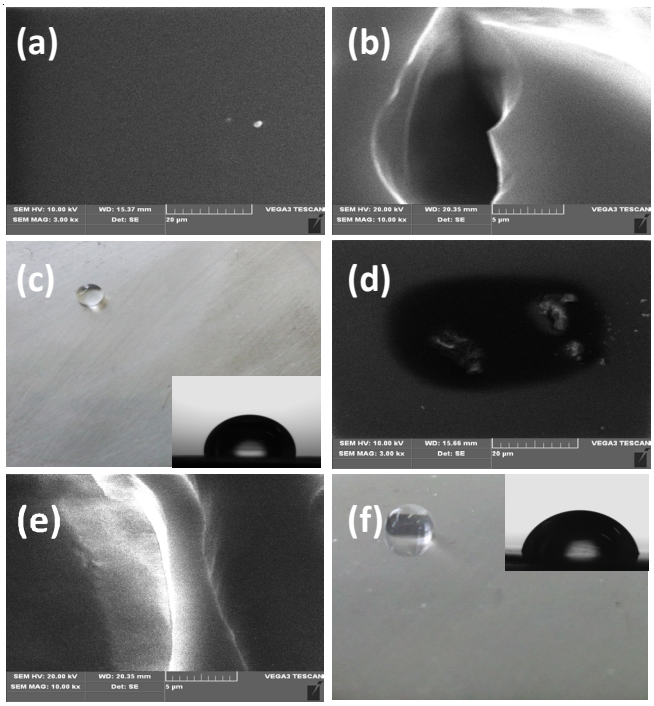

Fig. 6. SEM micrographs of nanocomposites modified by chemical grafting (a), (b), (c) and physical blend (d), (e), (f)

Transparent ZnO/silicone nancomposites were synthesized from component A and component B *via* hydrosilylation reaction. The UV-visible transmittance spectra of silicone and nanocomposites with different sizes (0.06 wt. % ZnO) are shown in Fig. 7a. The pure silicone resin has a high transmittance of visible-light and the optical properties are changed excellently by the different size of nano-ZnO. As the size of

ZnO increases, the transmittance of UV-light generally decreases. Though the samples calcined at 500 °C show outstanding UV-light shielding efficiency in Fig. 7a, the transparency is quite poor. The silicone/Z3 (0.06 wt %) exhibited a high and similar visible-light transparency as the pure silicone resin, but the former do not have very high UV-light shielding properties. However, the nanocomposites containing 0.06 wt % m-Z_4 nanoparticles calined at 400 °C exhibit not only show a high UV-light shielding (about 80 % at 280 nm and 32 % at 370 nm), but also high-visible light transparency.

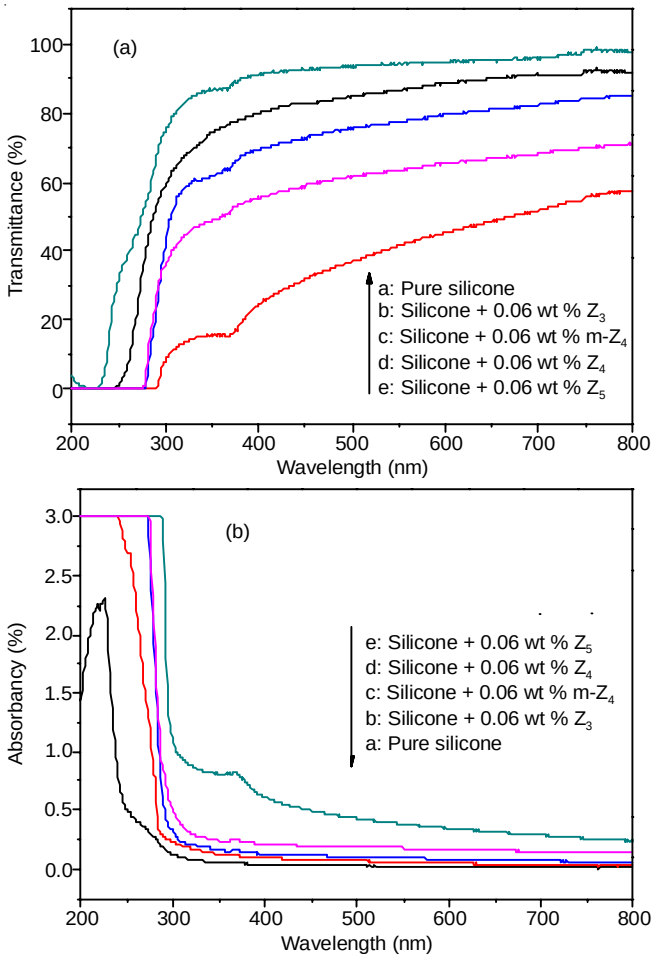

Fig. 7. UV-visible spectra of pure silicone and ZnO/silicone nanocomposites containing 0.06 wt % ZnO nanoparticles (a) transmittance and (b) absorbance

Additionally, Fig. 7b shows that UV-light absorbance of the nanocomposites increases generally with increasing calcination temperature. This agrees with the transmittance result (Fig. 7b). The absorbance curve of the composite based on other particles shows a sharp absorption peak at 375 nm, of which the intensity increased with increasing size of ZnO in the composite. This is attributed to the blue shift phenomenon caused by the quantum size effect of the nano-ZnO particles. Because the blue shift is negative for the UV-shielding, it is important to choose a suitable size of nano-ZnO.

The UV-shielding performance of the material is further verified *via* ultraviolet aging test and the change of material mechanics properties before and after test is displayed in Fig. 8. It can be seen from Fig. 8 that the mechanical properties of

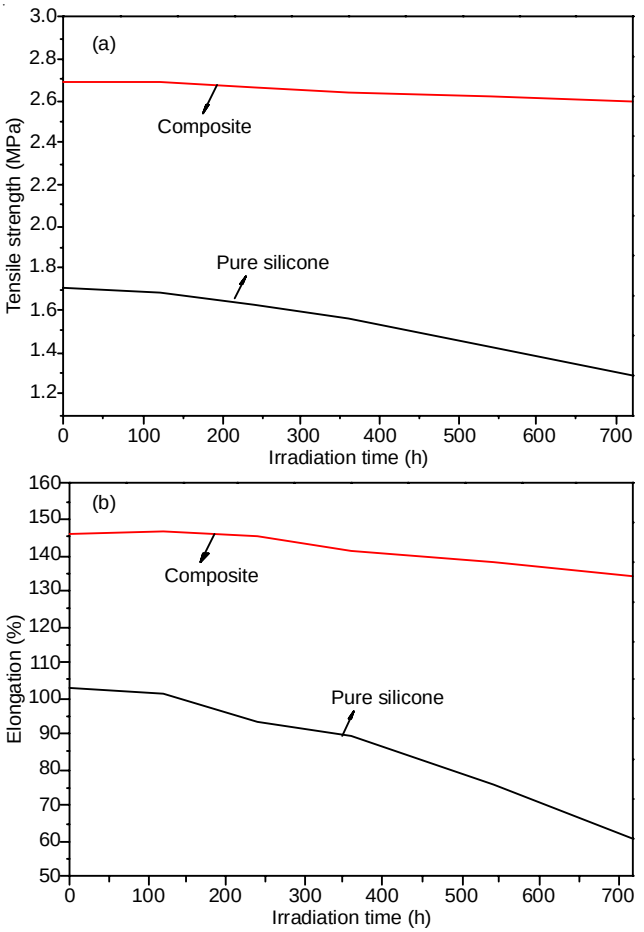

Fig. 8. Changes of the material properties *via* ultraviolet aging test

the pure silicone is declined significantly (the tensile strengthen declined from 2.23 mPa to 1.79 mPa and the elongation at break declined from 163 to 96 %) and a lot of silicone particles of the fracture surface are dropped after ultraviolet aging test for 750 h. One the contrary, the nanocomposites (contain with 0.06 wt % m-Z_4) is showed higher UV-shielding and stability than that of pure silicone. This is in agreement with the results in Fig. 7b.

ZnO nanoparticles as filler are not only a kind of light stabilizer, but also a thermal stabilizer that are exhibited excellent thermal properties. Fig. 9 displays the TG-DTA curve of pure silicone and nanocomposites (0.06 wt % m-ZnO). As shown TGA curves in Fig. 9, it clearly indicate that thermal properties of silicone are obviously changed by nano-ZnO in troduced. The temperature of the nanocomposites thermogravimetric 5 wt % to 456 °C is far higher than that of pure silicone (355 °C) and the nanocomposites is only weight loss 27 wt % at 525 °C. However, the pure silicone is almost decomposed completely at the same temperature. From DTA curves, it can also be proved that the maximum weight loss rate of nanocomposites is lower than that of pure silicone and this is very favorable for electronic packaging.

Additionally, the maximum weight loss rate of nanocomposites at 461 °C or less is 5 wt % since it mainly contains a small amount of small molecules and moisture. (2) The nanocomposites loss 65 wt % of its weight from 461 to 570 °C mainly because of the methyl and methylene bases of molecule mains are decomposed. Especially, temperature above at 520 °C,

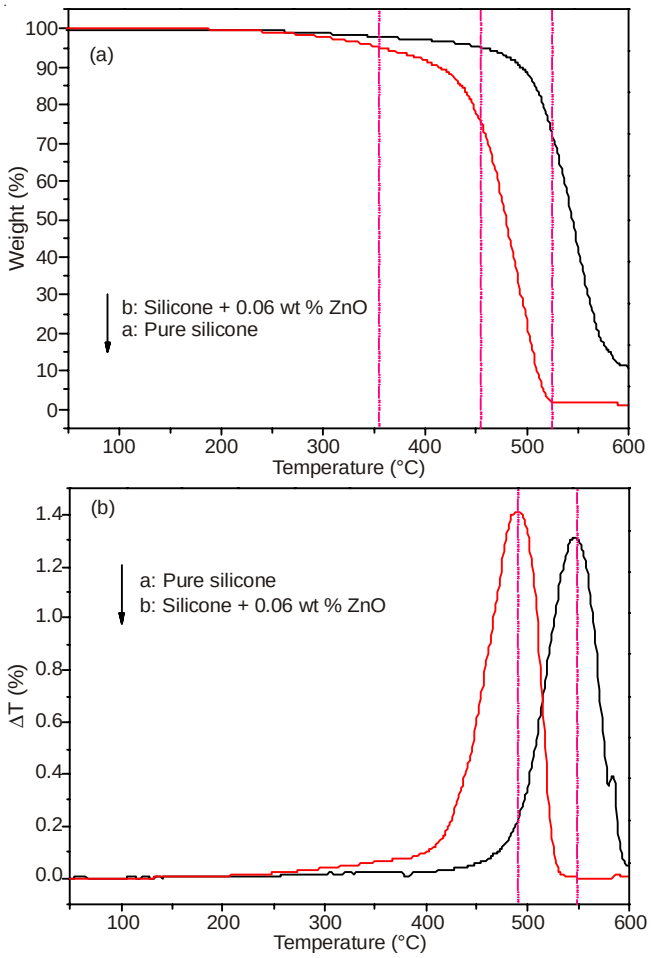

Fig. 9. TG-DTA cure of samples: (a) pure silicone and (b) nanocomposites

the 3d flight track of the polymer molecular silicone atoms and the oxygen atoms with adjacent unshared electrons are coordinated and then the Si-O-Si bases are fractured and formated a variety of siloxane under high temperature. As the temperature is above 570 °C, the nanocomposites slow down their speed of decomposition until it comes to a stable level. It can be proved by analysis that the introduction for the ZnO nanoparticles increased the initial decomposition temperature by 25 % and pyrolysis residues quality by 15 %, which will well meet the requirement of electronic products packaging.

Conclusion

In summary, novel transparent ZnO/silicone nanocomposites with excellent intergrafted properties, including a high UV-shielding efficiency, high-visible light transparency and high thermal properties were reported in this paper. ZnO precursor was synthesized *via* the homogeneous precipitation method and different nano-size ZnO particles were then obtained by calcination of the precursor at different temperatures. Transparent ZnO/silionce nanocomposites were successfully prepared by incorporation of factionalized ZnO nanoparticles in a transparent silicone and the effect of ZnO nanoparticles on optical and thermal properties of nanocomposites were investigated. The results showed that fictionalizations with A151 greatly improved the dispersion of ZnO in silicone due to their high chelating capacities with ZnO and good compatibilities with silicone and the refractive index of the nanocomposites were changed by m-ZnO chemical grafting. The transmittance of nanocomposites were reached above 80 % with 0.06 wt % m-ZnO nanoparticles (an average size of 96.01 nm after calcination at 400 °C). Moreover, the ultraviolet aging resistance, mechanical and thermal properties of silicone material were enhanced with m-ZnO introduced and met the requirements of high-performance electronic packaging for high-power light-emitting diodes encapsulant.

REFERENCES

1. S. Reineke, F. Lindner, G. Schwartz, N. Seidler, K. Walzer, B. Lussem and K. Strasse, *Nature*, **459**, 234 (2009).
2. S. Liu and X.B. Luo, *Chem. Ind. Press*, **26**, 1 (2011).
3. R. Zhang and S.W.R. Lee, *Microelectron. Reliab.*, **52**, 922 (2012).
4. Y. Zhou, N. Tran, Y.C. Lin, Y.Z. He and F.G. Shi, *Adv. Packaging*, **33**, 484 (2008).
5. Y. Morita, S.T. Tajima, H. Suzuki and H. Sugino, *J. Appl. Polym. Sci.*, **100**, 2010 (2006).
6. Y. He, J.A. Wang, C.L. Pei, J.Z. Song, D. Zhu and J. Chen, *J. Nanopart. Res.*, **12**, 3019 (2010).
7. X. Yang, W. Huang and Y.Z. Yu, *Appl Polym*, **120**, 1216 (2011).
8. S. Ma, W.Q. Liu, N. Gao, Z.L. Yan and Y. Zhao, *Macromolecular*, **19**, 972 (2011).
9. J.S. Kim, S.C. Yang and B.-S. Bae, *Chem. Mater.*, **22**, 3549 (2010).
10. Y.H. Lin, J.H. You, Y.C. Lin, N.T. Tran and F.G. Shi, *Compon. Packag. Technol.*, **33**, 761 (2010).
11. C.J. Hawker, H. Nulwala, A.A. Odukale, J.A. Gerbec and K. Takizawa, US Patent 8035236B2 (2011).
12. L.M. Liao, H. Liang, L. Chen and Z.Q. Wang, *Appl. Mechan. Mater.*, **423-426**, 1046 (2013).
13. Y. Liu, Z.Y. Lin, X.Y. Zhao, K.S. Moon, S. Yoo and C.J. Electron, *Compon. Technol. Confer.*, **5**, 553 (2013).
14. X. Ma, P.H. Zhang, Y. Fan and H. Chen, *Stratrgic. Technol.*, **9**, 1 (2012).
15. M. Zhang, K. Zhang, X.F. Zhang, C. Yang and M.M.F. Yuen, *Electron. Mater. Packag.*, **12**, 1 (2012).
16. Y.Q. Li, S.Y. Fu and Y.W. Mai, *Polymer*, **47**, 2127 (2006).
17. E. Tang, H. Liu, L. Sun, E. Zheng and G. Cheng, *Eur. Polym. J.*, **43**, 4210 (2007).
18. W. Zhang, Y. He, C.L. Pei, J.H. Song, D. Zhu and J. Chen, *Acta. Polym. Sinica*, **1406** (2010).
19. Y.P. Sun, A.J. Gu, G.Z. Liang and L. Yuan, *J. Appl. Polym. Sci.*, **121**, 2018 (2011).
20. F. Du, C. Guthy, T. Kashiwagi, J.E. Fischer and K.I. Winey, *J. Polym. Sci. Pol. Phys.*, **44**, 1513 (2006).
21. N. Samaele, P. Amornpitoksuk and S. Suwanboon, *Powder Technol.*, **203**, 243 (2010).
22. H.Q. Shi, W.N. Li, L.W. Sun, Y. Liu, H.M. Xiao and S.Y. Fu, *Chem. Commun.*, **47**, 11921 (2011).
23. N.C.S. Selvam, S. Narayanan, L.J. Kennedy and J.J. Vijaya, *J. Environ. Sci. (China)*, **25**, 2157 (2013).
24. B.D. Cullity, Elememts of X-Ray Diffraction, Addison-Wesley, New York (1987).
25. Y.Q. Qing, Y.S. Zheng, C.B. Hu, Y. Wang, Y. He, Y. Gong and Q. Mo, *Appl. Surf. Sci.*, **285**, 583 (2013).
26. Y.F. Wang, B.X. Li and C.Y. Xu, *Superlattices Microstruct.*, **51**, 128 (2012).
27. Y. He, J.A. Wang, C.L. Pei, J.Z. Song, D. Zhu and J. Chen, *J. Nanopart. Res.*, **12**, 3019 (2010).
28. W.J. Xu, J.L. Song, J. Sun, Y. Lu and Z.Y. Yu, *ACS Appl. Mater. Interf.*, **3**, 4404 (2011).
29. Y.N. Wang, *New Chem. Mater.*, **40**, 117 (2012).